frontiers | Frontiers in Earth Science

TYPE Original Research
PUBLISHED 16 January 2026
DOI 10.3389/feart.2025.1750309

Check for updates

OPEN ACCESS

EDITED BY
Xiaoping Zhou,
Chongqing University, China

REVIEWED BY
Zarghaam Rizvi,
GeoAnalysis Engineering GmbH, Germany
Fei Tan,
China University of Geosciences
Wuhan, China

*CORRESPONDENCE
Yiming Wang,
wzwym@wzu.edu.cn

RECEIVED 20 November 2025
REVISED 24 December 2025
ACCEPTED 30 December 2025
PUBLISHED 16 January 2026

CITATION
Zhou L, Ping Q, Shen H, Wang Y, Huang Q and Zhang D (2026) Experimental study on critical conditions of ground collapse caused by leakage of pressurized hydraulic pipelines in sandy formations.
Front. Earth Sci. 13:1750309.
doi: 10.3389/feart.2025.1750309

COPYRIGHT
© 2026 Zhou, Ping, Shen, Wang, Huang and Zhang. This is an open-access article distributed under the terms of the Creative Commons Attribution License (CC BY). The use, distribution or reproduction in other forums is permitted, provided the original author(s) and the copyright owner(s) are credited and that the original publication in this journal is cited, in accordance with accepted academic practice. No use, distribution or reproduction is permitted which does not comply with these terms.

Experimental study on critical conditions of ground collapse caused by leakage of pressurized hydraulic pipelines in sandy formations

Liling Zhou[1,2,3], Qimeng Ping[4], Huizhen Shen[1,2,3], Yiming Wang[4,5]*, Qing Huang[1,2,3] and Dazheng Zhang[1,2,3]

[1]Zhejiang Institute of Geosciences, Hangzhou, China, [2]Observation and Research Station of Zhejiang Coastal Urban Geological Security, Ministry of Natural Resources, Hangzhou, China, [3]Qiantang Institute of Geology, Hangzhou, China, [4]College of Civil Engineering and Architecture, Wenzhou University, Wenzhou, China, [5]Zhejiang Engineering Research Center of Disaster Prevention and Mitigation for Coastal Soft Soil Foundation, Wenzhou, China

Ground collapse poses a significant threat to urban safety, and pipeline leakage in sandy formations is an important factor that triggers it. A series of physical experiments was designed to explore the process, especially the critical conditions of ground collapse caused by leakage of pressurized water pipes. According to the test results, under different combinations of compactness of sand and water flow velocity in the pipeline, three final states of sandy formations under pipeline leakage erosion were identified: infiltration disturbance, stable cavity, and fluidization failure. Then, the critical conditions between the state of stable cavity and fluidized failure were obtained, which can be used for predicting ground collapse caused by pipeline leakage. Thirdly, a model for predicting the scale (volume and area) of ground collapse was built by logarithmic regression analysis. Finally, a ground collapse early warning model was proposed based on the correspondence between surface subsidence monitoring data and the area of cavities in the sandy formation during the experimental process. The research results can serve as a scientific basis for the prevention and control of urban ground collapse.

KEYWORDS

early warning, fluidization failure, ground collapse, infiltration, monitoring

1 Introduction

Ground collapse is a major type of geological disaster (Hou et al., 2013). Because of its characteristics of suddenness and concealment (Yuan, 2014), ground collapse poses a great threat to pedestrians and vehicles in cities (Hermosilla, 2012; Hu et al., 2016). For example, in Shenzhen, China, a total of 1430 ground collapse accidents occurred between 2016 and 2020, causing certain casualties and significant economic losses, resulting in a total of 7 deaths and property losses of approximately 238.225 million yuan (Shi et al., 2022). Ground collapses may concentrate and occur in the same area or at a certain time period, forming disasters. For example, from June 11 to July 18, 1995, dozens of ground collapses occurred near Aigang Village, Renhe Town, Baiyun District,

Guangzhou City, China (Liu et al., 2007). Ground collapse may also occur repeatedly. For example, since the completion of pipeline laying in 2003, the ground collapse on Haitai East Road in Tianjin has collapsed 4 times, interval of every 1.5–2 years. And although it has been treated multiple times, the ground collapse still continues (Mao and Huang, 2014).

The formation of ground collapse is influenced by both natural and human factors. Some scholars believe that most of the ground collapse is formed by natural factors (Kuliczkowska, 2016). Some others, however, felt that human engineering disturbances play a significant role in triggering ground collapse in densely populated urban areas (Tan and Long, 2021). Among so many human engineering disturbances, the majority of road surface collapse is due to leakage caused by defects in sewage pipes (Mukunoki et al., 2009). Paolo Maria Guarino et al. believed that the main triggering mechanism for ground collapse caused by human factors is the saturation of the subsoil due to underground sewage and water pipeline leaks (Guarino et al., 2018). Liu J and other scholars found that the collapses caused by defects in shallow buried pipelines account for approximately 63.9% of the total road surface collapses, based on statistics (Liu et al., 2024).

In order to study the process and mechanism of ground collapse caused by pipeline leakage, scholars have conducted a large number of physical experiments. Fei Tan et al. conducted indoor model experiments to directly observe the process of pipeline leakage and collapse, revealing the important significance of cavity evolution in predicting ground collapse (Tan et al., 2022). F. Zoueshtiagh and A. Merlen studied the response of a granular bed to a vertical jet below it from experimental, theoretical, and numerical perspectives, and outlined the behavior of the bed in three states depending on the flow rate Q (Zoueshtiagh and Merlen, 2007). Controlled laboratory-scale experiments have been widely used to investigate threshold-driven responses of subsurface materials under sustained and cyclic forcing, allowing direct observation of progressive disturbance and failure mechanisms that are difficult to capture in field conditions (Ahmad et al., 2019; Ahmad et al., 2021). Zhang, Sulei, et al. studied the failure behavior of composite strata caused by tunnel excavation under seepage conditions due to pipeline leakage using indoor model experiments and the finite difference method (Zhang et al., 2022). D Zi Li, et al. designed a model experimental device to study the evolution law of the soil erosion zone and collapse pit caused by underground hydraulic pipeline leakage. They quantitatively analyzed the characteristics of pore water pressure and surface displacement changes caused by pipeline leakage through pore water pressure sensors and displacement sensors, and explored the influence of four factors: water flow velocity inside the pipeline, pipeline burial depth, initial soil moisture content, and defect location on soil erosion process and collapse pit morphology (Dai et al., 2024). A simplified model was proposed based on the flow channel boundary and ground settlement profile during the process of water flow through model experiments, and the effectiveness of the model was verified through indoor fine sand and medium sand model experiments (Zheng et al., 2016). Jixiang Guo et al. designed a fracture collapse model test device and used digital image correlation (DIC) technology to study the erosion process and collapse mechanism of underground pipeline leakage. Artificial groundwater seepage provided the driving force for collapse, and defects provided migration space, which together caused collapse (Guo et al., 2024).

In recent years, numerical simulation, artificial intelligence, and other numerical methods have been widely applied in the formation process and mechanism of ground collapse. Ahmad Momeni et al. proposed a direct, data-driven, artificial intelligence prediction tool for leak localization and severity measurement (Momeni et al., 2023). Xueyang Yuan et al. used the Discrete Element Method (DEM) to study the mechanism of ground collapse in dry sand layers and water-rich sand layers, and believed that water pressure was the main factor affecting the PLR of the pipe column (Yuan et al., 2025). Xilin Cui et al. conducted a numerical study on soil fluidization caused by local leakage in buried pipelines using the Discrete Element Lattice Boltzmann Coupling Method (DEM-LBM), and established the relationship between fluidization pressure, pipeline burial depth, and leakage size (Cui et al., 2014). Hao Tong Zhou et al. used a coupled method of computational fluid dynamics and discrete element method (CFD-DEM) to numerically simulate the development process of drilling subsidence disasters caused by groundwater flow, and studied the laws and characteristics of formation deformation and foundation loss (Zhou et al., 2022). In parallel with physical and numerical modeling, data-driven and machine-learning approaches have been increasingly used to identify degradation trends and critical thresholds in geotechnical systems, particularly for prediction and early-warning purposes based on monitored response data (Ahmad et al., 2025a).

Through physical experiments and numerical simulations, scholars have analyzed the process, mechanism, and influencing factors of ground collapse caused by pipeline leakage. For the process of ground collapse induced by pipeline leakage, scholars generally divide it into three stages: slight disturbance (mild), formation of cavities (moderate), and soil fluidization (severe). From a micromechanical perspective, progressive bond degradation and localized instability can lead to sudden loss of load-bearing capacity once a critical state is reached, as demonstrated in lattice-based modeling of geomaterials (Rizvi et al., 2020). Existing research suggests that the water flow formed by pipeline leakage causes erosion and disturbance to the water flow around pipeline defects. The migration of a large number of fine particles and the aggregation of coarse particles around the defective pipeline led to the formation and expansion of temporary cavities, which is believed to be the mechanism of ground collapse. Geometric characteristics of subsurface openings significantly influence stress redistribution and stability, with shape-dependent failure behavior reported in experimental and numerical studies of underground openings (Alsabhan, 2021). Among the numerous natural and human factors that affect ground collapse, soil parameters, fluid pressure, pipeline burial depth, and leakage size have a significant impact on the formation of ground collapse.

Although there have been many research achievements in the field of ground collapse caused by pipeline leakage, there are still shortcomings in the mechanism and formation conditions of ground collapse, which pose difficulties and challenges for the prediction and prevention of such disasters. For example, previous studies have mostly focused on the process of soil fluidization failure, but have not conducted detailed research on the critical conditions

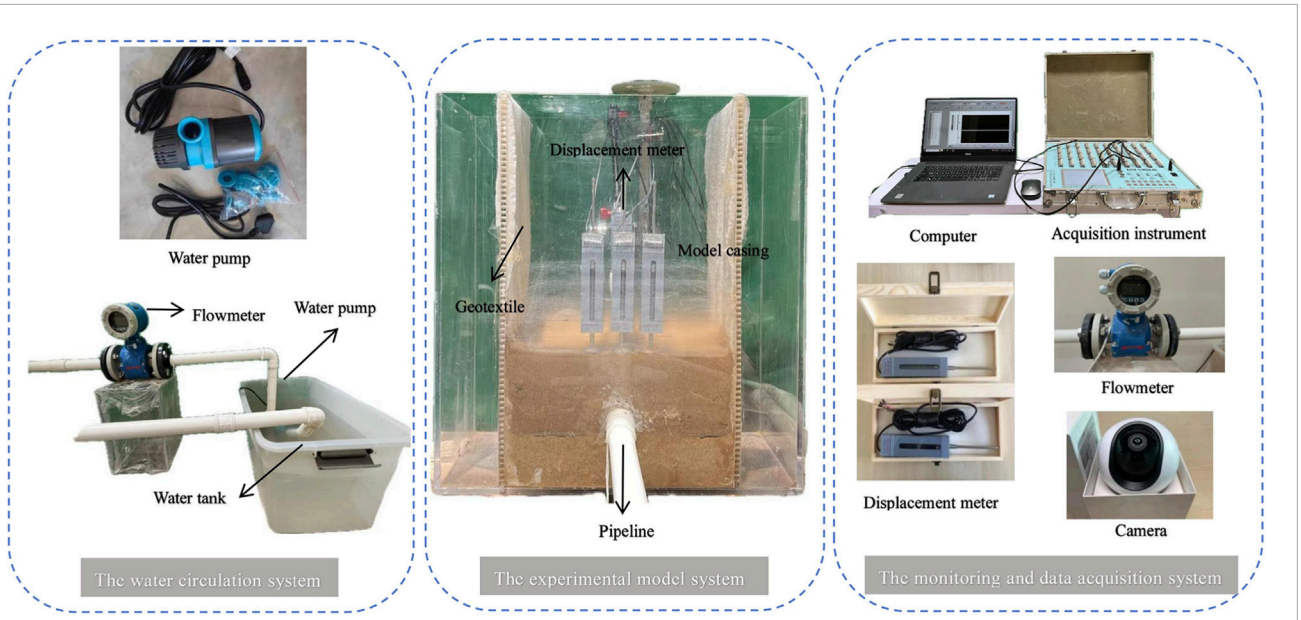

FIGURE 1
Composition of experimental device system.

under which it occurs, and this is crucial in ground collapse monitoring and early warning. Recent experimental investigations highlight that soil systems subjected to localized energy input may exhibit nonlinear responses and abrupt transitions once critical thresholds are exceeded, underscoring the need for quantitative identification of governing failure conditions (Ahmad et al., 2025b). This article conducted a series of experiments on ground collapse caused by pipeline leakage, identified three final states of soil under pipeline leakage erosion, as well as the critical conditions for such ground collapse. A prediction model for the scale of ground collapse and a monitoring and early warning model was established, which can provide scientific basis for the prevention and control of urban ground collapse.

2 Model test methods

2.1 Test apparatus

A test apparatus was developed to simulate ground collapse caused by leakage of pressurized hydraulic pipelines in sandy formations. The experimental apparatus consists of three parts: the experimental model box, the water circulation system, and the experimental monitoring and data acquisition system (Figure 1).

The experimental model system was made of organic transparent glass, with a length of 600 mm, a width of 300 mm, and a height of 700 mm. The model box adopts a semi-structured mode, and the experimenters can observe the process of sand loss and the development status of underground cavities through the transparent side. There were two porous plates at both ends inside the model box, which were fixed to the model box with glass glue. Each board had multiple overflow holes with a diameter of 0.5 cm, which were used to simulate water infiltration outward. Geotextiles were covered near the porous plate on the soil side to prevent sand from flowing out of the porous plate. To reduce boundary effects, the side walls of the model box were made of smooth and transparent acrylic sheets, and porous plates and geotextiles were set up to simulate semi-infinite soil conditions.

The water circulation system was connected to the model box through water pipelines. The outer diameter of the pipeline was 40 mm, with a wall thickness of 2 mm. One side of the water pipeline was connected to a variable frequency water pump and flow meter. On the other side of the water pipeline, a damaged opening with a diameter of d_0 = 15 mm was pre-set near the edge of the model box to simulate pipeline defects. The buried depth of the pipeline in the model box was 100 mm, and the minimum burial depth of the pipeline (h_p) design in the experiment was 100 mm, d_0/h_p = 0.15 < 0.2; the burial depth of the pipeline met the assumption of a point source jet. The pressurized hydraulic pipeline system mainly included a variable frequency water pump and a water storage tank, which collected the water discharged from the inlet pipeline through the water storage tank. At the same time, the variable frequency water pump was adjusted by variable frequency to change the inlet flow rate of the inlet pipeline, and the erosion of soil caused by pipeline damage under different hydraulic conditions was studied.

The monitoring and data acquisition system mainly included flow meters, displacement sensors, camera instruments, and a data acquisition instrument. The flowmeter was used to monitor the flow rate at the inlet, and through calculation, it can be determined whether the flow rate at the inlet meets the design requirements. Displacement sensors were used for soil subsidence data. The data acquisition instrument converted the electrical signals generated by strain into digital signals through the data acquisition instrument, and collected data through a computer.

10.3389/feart.2025.1750309

TABLE 1 Experimental programs.

Case	Compactness of sand (%)	Flow velocity (m/s)	Case	Compactness of sand (%)	Flow velocity (m/s)
1	0.2	1.34	19	0.425	1.34
2		1.42	20		1.42
3		1.5	21		1.5
4		1.55	22		1.55
5		1.62	23		1.62
6		1.69	24		1.69
7	0.275	1.34	25	0.5	1.34
8		1.42	26		1.42
9		1.5	27		1.5
10		1.55	28		1.55
11		1.62	29		1.62
12		1.69	30		1.69
13	0.35	1.34			
14		1.42			
15		1.5			
16		1.55			
17		1.62			
18		1.69			

2.2 Test scheme

To explore the critical conditions for ground collapse caused by pipeline leakage, the experiment was designed by controlling sand parameters and hydraulic conditions. The experiment selected the compactness of sand and the water flow velocity inside the pipeline for systematic research. The sand was set to five different degrees of compactness (Dr = 0.2–0.5). During the experiment, the prepared sand sample was filled into the model box in 5 layers using the rain method according to the compactness requirements, with each layer being 3 cm to ensure the compactness was the same. Hydraulic conditions were regulated by variable frequency water pumps to adjust the flow rate (v = 1.34 m/s~1.69 m/s). A total of 30 model experiments were conducted in this experiment, and the specific experimental plan was designed as shown in Table 1.

It is worth mentioning that in order to explore the triggering boundary (including flow velocity) of ground collapse induced by underground pipeline leakage, more than 10 attempts were made at the earlier stage. Only after determining the approximate parameter range, these 30 physical experiments carried out.

The geometric similarity ratio of this experiment is 1:10. According to the "Design Standard for Outdoor Water Supply" (GB50013-2018), the minimum soil cover depth of the water supply pipeline under the motor vehicle lane should not be less than 0.70 m. The prototype soil cover for this experiment is 1.0 m, corresponding to a model burial depth of 100 mm. The size of the damaged opening meets the assumption of point source jet. The soil was selected from river sand and sieved according to similarity ratio to ensure that the particle mechanical behavior was similar to the prototype (Table 2). For the convenience of the experiment, Sand with particle sizes too large (>2 mm) or too small (≤0.075 mm) was screened out. Excessive particle size of sand may cause blockage and affect the test process, while a small particle size of sand is not conducive to the collection and reuse of soil. The particle size distribution curve of the test soil sample is shown in Figure 2.

3 Model test results

3.1 Three final states of the experiment

Among the 30 experiments, the test results can be divided into three stable states based on the test results: infiltration disturbance,

TABLE 2 Major physical parameters of the soil samples.

Parameter	γ_{dmax} (KN/m^3)	γ_{dmin} (KN/m^3)	G_s	e_{max}	e_{min}	d_{50} (mm)	d_{90} (mm)	C_u	C_c
Value	1.731	1.442	2.63	0.824	0.519	0.385	0.898	2.92	1.23

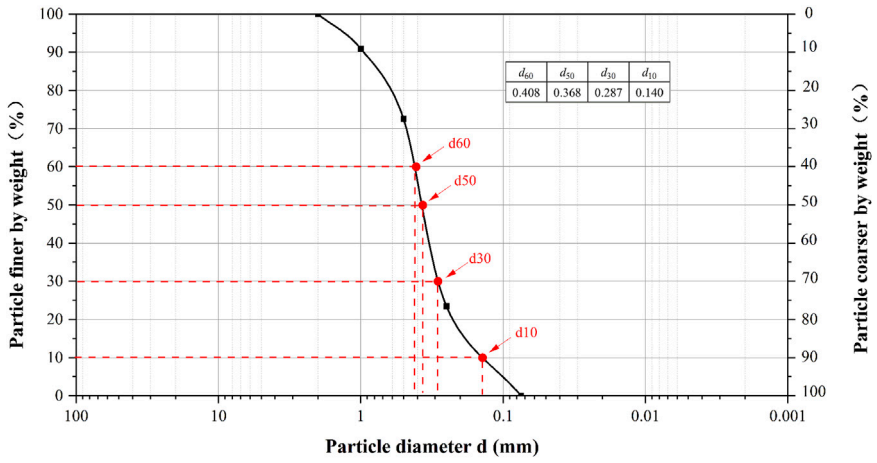

FIGURE 2
The particle size distribution curve of the test soil.

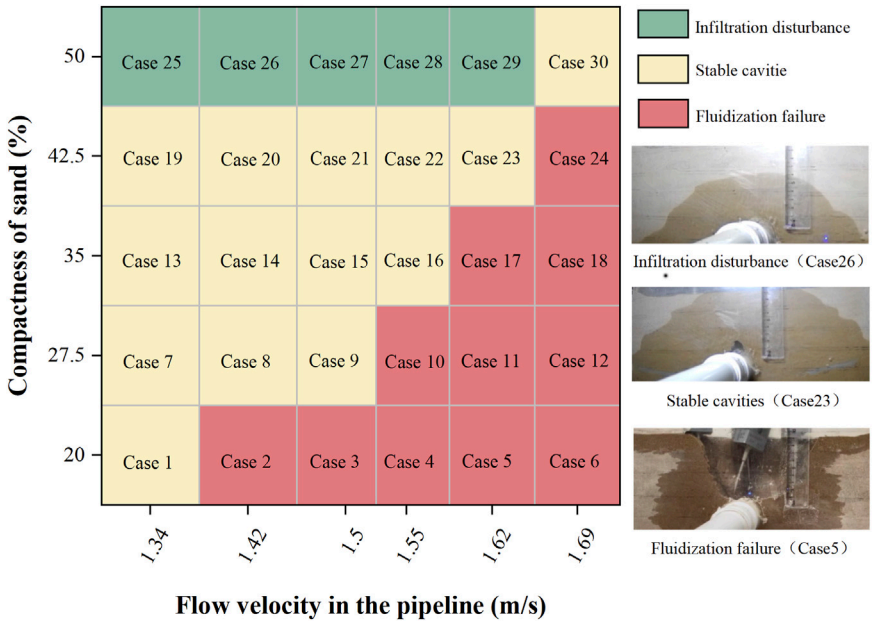

FIGURE 3
Three final states of the experiments.

stable cavities, and fluidization failure (Figure 3). These three states can be maintained for more than 24 h.

When the soil was relatively dense and the velocity of seepage flow was lower than a certain limit, the soil was only slightly disturbed, which was mainly manifested as the water infiltrating part of the sand. When the compactness of sand decreased slightly and the velocity of seepage flow was limited within a certain range, the soil was disturbed to a large extent, showing obvious cavities and maintaining relative stability. When the compactness of sand was small and the velocity of seepage flow was greater than a certain limit, the soil would be seriously disturbed, and it would be difficult to maintain stability, and fluidization collapse would occur.

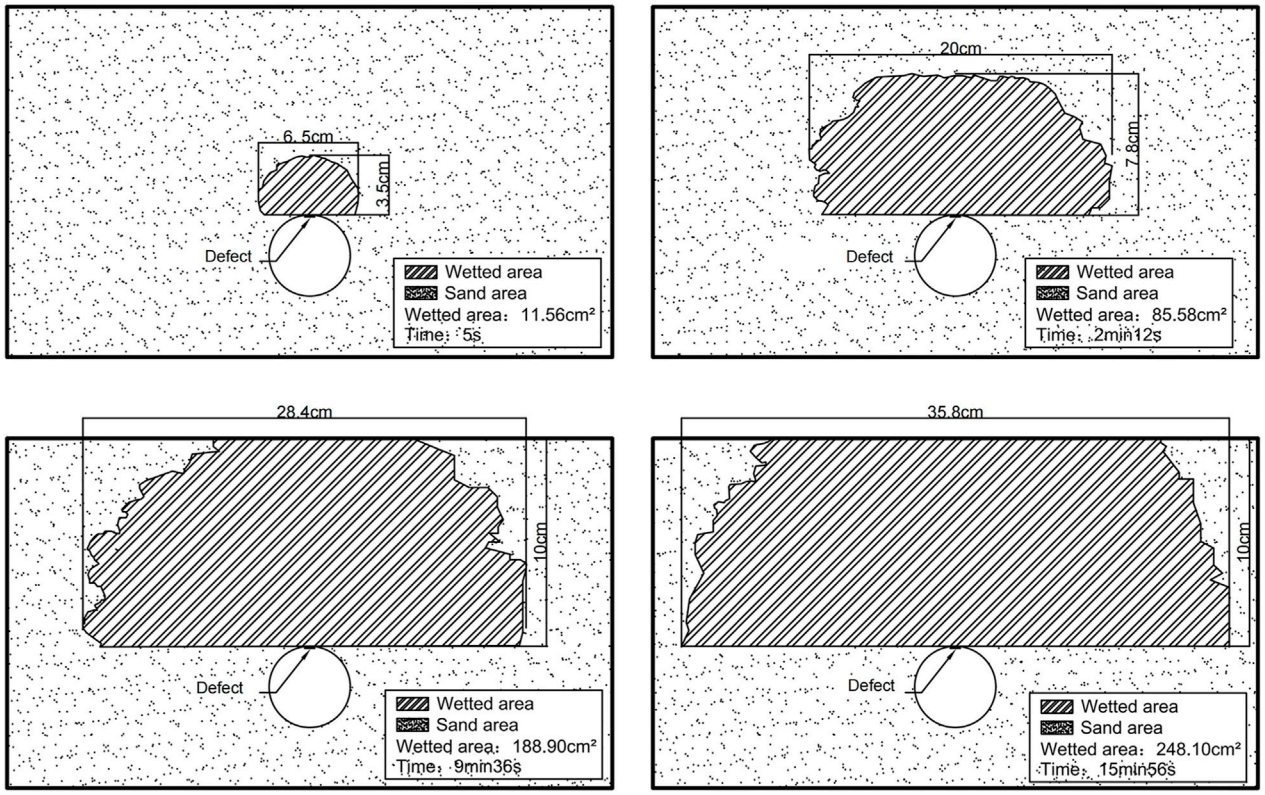

FIGURE 4
Schematic diagram of infiltration area evolution (case 10).

3.2 Infiltration disturbance

The state of infiltration disturbance mainly occurs when the flow velocity of the leaking water is low and the compactness of sand is high (Dr ≥50%, and water ≤1.62 m/s).

In the initial stage of the experiment, the water flow from the defect above the pipeline seeped into the soil at a relatively fast speed. Water flowed through soil pores under a certain pressure gradient, and the infiltration line generally spread uniformly in an elliptical shape, with the relatively constant eccentricity between 0.9 and 0.95, indicating that the infiltration of water in the soil was homogeneous. In this state, the soil did not show significant deformation, mainly manifested as water infiltration (Figure 4).

Soil infiltration can be roughly divided into two stages (Figure 5). At the initial stage, the phreatic line expanded rapidly, and its height and width rose rapidly. The initial infiltration rate was about 0.37 cm^2/s. Then the expansion speed of the phreatic line slowed down significantly, and the infiltration rate in this stage was about 0.26 cm^2/s. The average rate of the infiltration front advancement was approximately 0.3 cm^2/s. Compactness of sand and flow velocity both had significant effects on infiltration range and velocity. The compactness of sand was inversely proportional to the scope of infiltration and the velocity, while the velocity of water flow was directly proportional to it. The smaller the compactness of sand and the faster the water flow rate, the faster the expansion speed and rise speed of the infiltration line.

3.3 Stable cavities

When the compactness of sand and the seepage velocity of water flow are limited within a certain range (such as Dr <50%, while V_w ≤1.62 m/s, or Dr ≥50%, while V_w ≥1.69 m/s), cavities appear inside the soil and remain relatively stable for more than 24 h.

Under the above conditions, a clear taper cavity formed quickly above the defect opening of the pipeline at the initial stage of the experiment. As the water flow continued to erode, many small erosion points appeared on the periphery of the cavity, expanding gradually and finally connecting to form an erosion zone at the edge of the cavity, and the cavities became larger and semi-circular. If the conditions were appropriate, these cavities may remain stable, with the sizes ranging from 0.38 cm^2 to 9.8953 cm^2 (Figure 6).

3.4 Fluidization failure

When the compactness of the soil and the seepage velocity of the water flow exceed a certain limit range (Dr < 50%, or V_w ≥ 1.42 m/s), the semi-circular cavity formed by water flow erosion cannot maintain stability and will continue to change, ultimately leading to fluidization failure. Fluidization failure refers to the inability of sand to maintain stability under water flow erosion, which continues to evolve within 24 h until failure occurs. At this point, sand loses its structural strength under water flow erosion and ultimately undergoes flow failure.

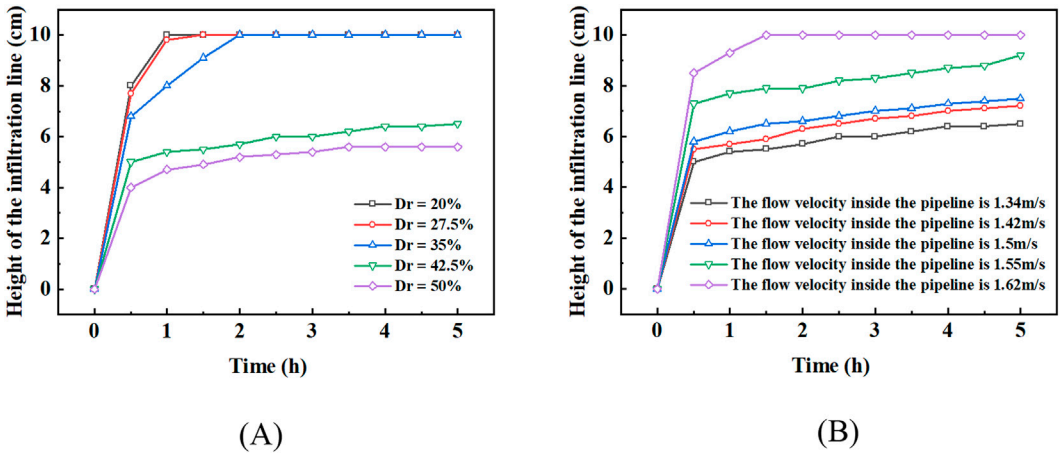

FIGURE 5
Variation of infiltration height under different soil compactness and flow velocity. **(A)** The compactness of the soil remains unchanged. **(B)** The flow velocity remains constant, with the flow velocity inside the pipeline varies with the soil density varies.

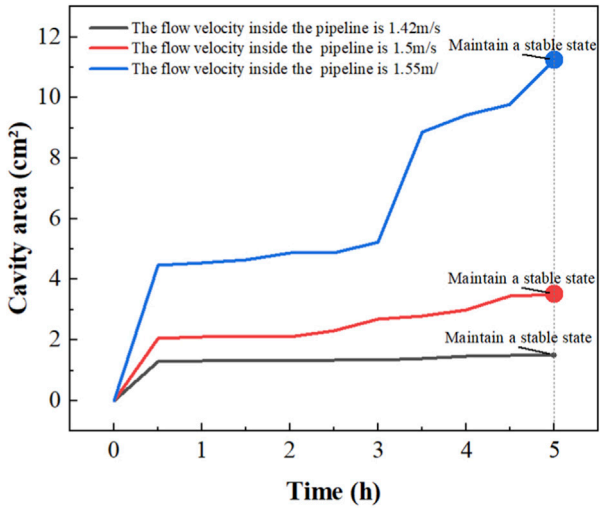

FIGURE 6
Evolution of void area under the same soil density and different flow velocities.

In these cases, the soil cannot resist the erosion force of water flow, and the cavities in the soil would be difficult to maintain stability and continue to develop. The cavities first continued to develop upward along the direction of flow erosion, and the shape gradually changed into a triangle, and then the top would be further eroded and expanded to form a rectangle. When the upward impact force of the water flow at the damaged outlet reached the limit, the scouring of the water flow gradually turned to lateral, the erosion effect of water at the top of the cavity was dominated by lateral expansion on both sides, and the cavity shape changed to a "T" shape, until the fluidization failure stage.

At the fluidization failure stage, the washed soil loses its strength and turns into a fluid state, eroding the cave wall with the water flow. With the continuous increase of the span at the top of the cavity, the overall stability of the soil continued to weaken, gradually lost its resistance to water erosion. Especially when the shape of the cavities changed to T-shape, the area of the suspended soil overlying the cavities increased abruptly, and the overlying soil without support was prone to collapse under the dual effects of self-weight and flow erosion. When the cavities could not support the pressure of the overlying soil, the soil collapsed as a whole. Macroscopically, it was shown as ground collapse (Figure 7).

4 Discussion

4.1 Critical condition of ground collapse caused by leakage of the pressure pipe

From the results of the above 30 tests, the transition from the state of stable cavities to fluidization failure is the turning point of the overall failure of the soil mass, so it is also the critical condition for the ground collapse caused by pipeline leakage. The compactness and velocity indexes corresponding to the boundary between the state of stable cavities and the fluidization failure were selected, and the regression analysis was carried out based on these indexes. Then, the early warning model of ground collapse caused by pipeline leakage was constructed (Figure 8).

A logarithmic function model was used to fit the relationship between the compactness of sand and flow velocity inside the pipeline. The fitting curve relationship is shown in Figure 9, and the fitting formula is as follows:

$$v = Aln(Dr) + B \quad (1)$$

In the formula, Dr is the compactness of the soil, and v is the water flow velocity. A and B are both fitting parameters, and the parameters A = 0.3639 and B = 0.2643 were obtained through experimental data fitting. Equation 1 can fit the relationship between the compactness of sand and flow velocity inside the pipeline. This formula represents the critical flow velocity that triggers fluidization

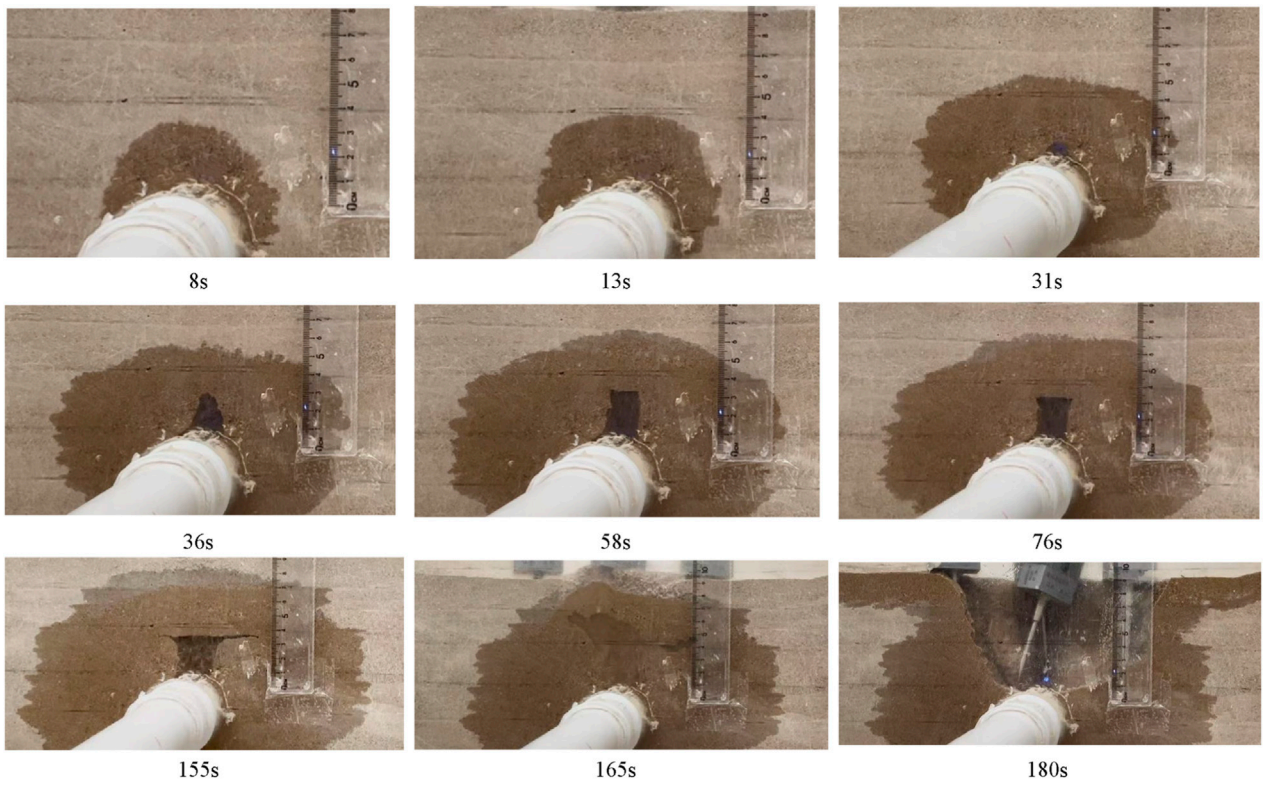

FIGURE 7
Variation of infiltration height under different compactness of sand and flow velocity. The compactness of the soil remains unchanged. The flow velocity remains constant cavity morphology evolution (case 12), with the flow velocity inside the pipeline varying with the compactness of the sand.

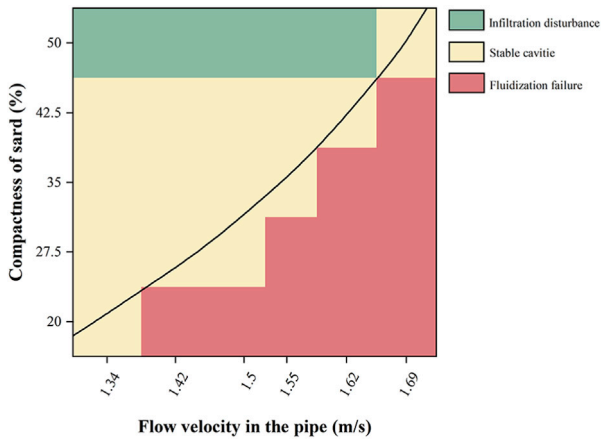

FIGURE 8
Diagram of critical state of test results.

failure in sandy soil at different compactness. It shows that with the increase of compactness of sand, the critical flow velocity increases, but the growth rate gradually slows down. The fitting results show that fluidization failure is similar to quicksand caused by groundwater seepage. The formation condition of quicksand is the critical hydraulic gradient, which is proportional to the compactness of sand. According to Darcy's law, the hydraulic gradient in soil is proportional to the flow velocity. So in quicksand, the water flow velocity is proportional to the compactness of the soil. The value of R^2 is 0.9825, indicating that the predicted results of the model have minimal deviation from the true values.

When the measured value is above this fitting curve, it means that the combination of compactness of sand and the flow velocity in the pipeline exceeds the bearing capacity of the soil, and this situation carries the risk of ground collapse. Therefore, this area can be considered a hazardous area. Accordingly, the soil mass can remain relatively stable in the area below the fitting curve.

Through the fitting curve, the flow velocity threshold corresponding to soil with different compactness of sand can be obtained, as shown in Table 3. Therefore, in practice, we can predict the risk of ground collapse caused by the damage of the pressurized water pipe through the relationship between the soil with a certain compactness and the flow velocity through the damaged water pipe.

4.2 Prediction of ground collapse scale

By analyzing the final shape and test conditions (compactness of sand and flow velocity in the pipeline) of the collapse pit caused by fluidization failure, it was found that there is an obvious corresponding relationship between the size of the collapse pit and the compactness of sand. As shown in Figure 10, the erosion angle of the collapse pit is positively correlated with the compactness of

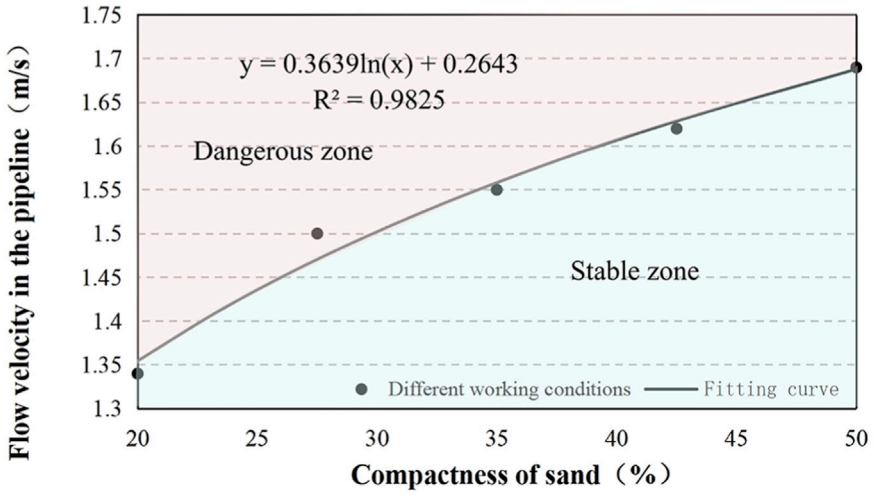

FIGURE 9
Fitting critical curve between soil compactness and velocity in pipeline.

TABLE 3 Water flow velocity threshold corresponding to the compactness of sand.

Compactness of sand (%)	20	25	30	35	40	45	50
Allow the water flow to erode at a certain speed (m/s)	1.355	1.433	1.502	1.563	1.607	1.649	1.688

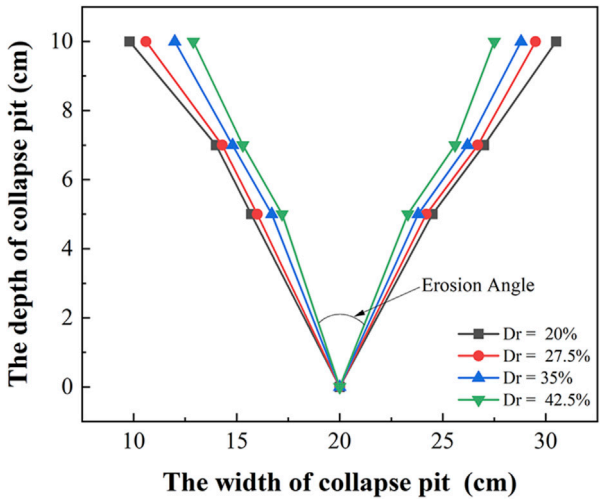

FIGURE 10
Collapse pit morphology of with different soil compactness.

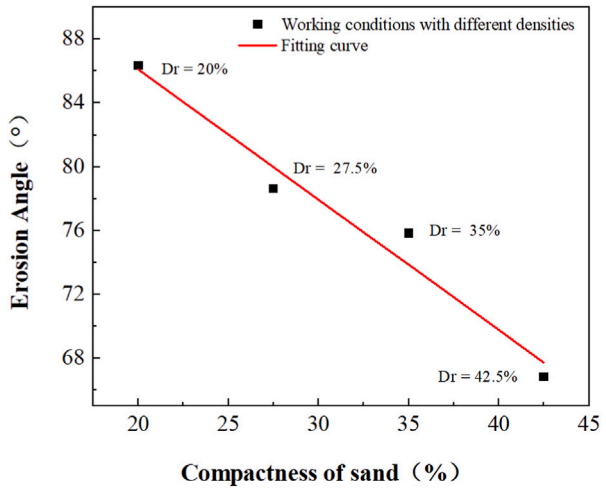

FIGURE 11
Fitting curve of soil density and collapse pit erosion angle.

sand, and the higher the compactness of the soil, the greater the erosion angle.

The linear function model was used to fit the relationship between compactness of sand and erosion angle, and it was found that the two have a good linear relationship. The fitting curve is shown in Figure 11, and the fitting formula is as follows (Equation 2):

$$\theta = A + BDr \quad (2)$$

Where θ is the erosion angle. Both A and B are fitting parameters, and the parameters A = 102.4567 and B = −0.8173 are obtained by fitting the test data. The value of R^2 is 0.9662, which shows that the model has a good fit.

On the basis of experimental observation and collapse cases, the instantaneous erosion pit shape of ground collapse is simplified into a normal cone (Figure 12). At the same time, it is assumed that the soil around the erosion pit is homogeneous, so as to ensure that the

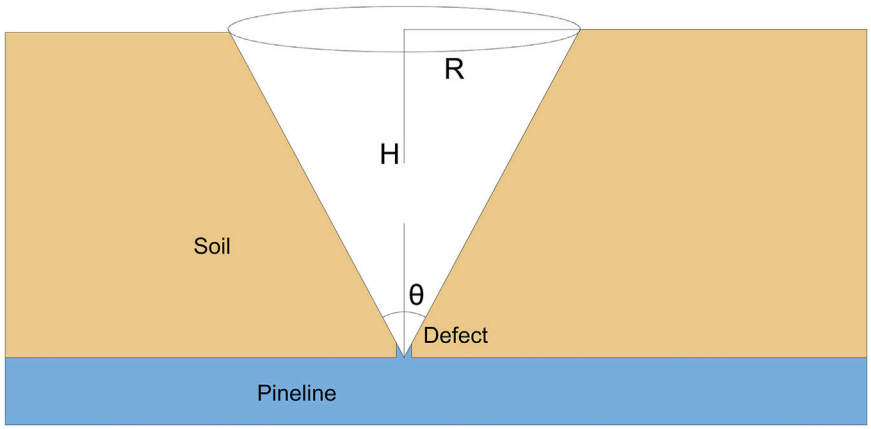

FIGURE 12
Simplify the schematic diagram of the erosion pit.

erosion angle (θ) of the pit wall on each side of the collapse pit is uniform, which can be described by a single angle.

By analyzing the relationship between compactness of sand and erosion angle, a prediction model for ground collapse volume and surface area based on compactness of sand and collapse depth can be obtained (Equations 3, 4).

$$V = (\pi H^3) tan^2(51.23 - 0.4085Dr)/3 \quad (3)$$

$$S = \pi H^2 tan^2(51.23 - 0.4085Dr) \quad (4)$$

Where V is the predicted volume of the ground collapse pit, S is the predicted area of the ground subsidence pit, and H is the depth of the ground collapse pit. According to the above formula, the scale of possible ground collapse (collapse volume and collapse area) can be predicted based on the compactness properties of the soil and the depth of the defective pipeline. It is worth noting that due to the complexity of the actual site rock and soil structure and hydrogeological conditions, the ground collapse induced by pipeline leakage is often not a perfect cone, so its impact range needs to be further refined and determined based on the site geological conditions.

4.3 Monitoring and early warning of ground collapse

As one of the effective monitoring methods for ground collapse, surface subsidence monitoring is widely used.

From the comparison chart of ground subsidence monitoring and underground cavity area (Figure 13), it can be seen that during the cavity development stage, the gradual development of surface subsidence corresponded to the increase in underground cavity area, and the growth trend of the two is almost synchronous. In the final stage of the experimental section, approaching the stage of fluidization failure, there is a clear critical point in both the surface subsidence curve and the underground cavity area curve. The trend of changes in the area of underground cavities was slightly ahead of the sudden change in ground subsidence, indicating the causal relationship between the development of underground cavities and ground subsidence. Afterwards, the surface subsidence and underground cavity area increased rapidly until fluidization failure occurred.

By comparing and analysing the monitoring data of critical surface subsidence before soil fluidization failure with the area of underground cavities, it was found that there was a corresponding relationship between surface subsidence and underground cavities (Tables 4, 5).

Using a binary linear function to fit and analyse the cavity area, subsidence, and pipeline flow velocity, the fitting plane is obtained as shown in Figure 14, and the fitting formula is as follows (Equation 5):

$$S = A + BH + Cv \quad (5)$$

Where S is the area of the cavity, H is the surface subsidence, and v is the water flow velocity. A. B and C are both fitting parameters, A = −18.34835, B = 0.6604, and C = 19.57515 were obtained through experimental data fitting. The value of R^2 is 0.9986, which shows that the model has a good fit.

Similarly, a binary linear function was used to fit and analyse the cavity area, subsidence, and compactness of sand, and the fitting plane was obtained as shown in Figure 14. The fitting formula is as follows (Equation 6):

$$S = A + BH + CDr \quad (6)$$

Where Dr is the Compactness of sand. A, B, and C are all fitting parameters, and A = −6.9255, B = 5.0242, and C = 0.0768 were obtained through experimental data fitting. The value of R^2 is 0.9999, which shows that the model has a good fit.

By slightly modifying Equations 5, 6, the critical surface subsidence under different compactness of sand and pipeline flow velocity can be obtained (Equations 7, 8), which can be used as the warning threshold for ground collapse monitoring equipment under corresponding working conditions.

$$H1 = -27.78 - 1.51S + 29.64v \quad (7)$$

$$H2 = 1.38 + 0.2S - 0.015CDr \quad (8)$$

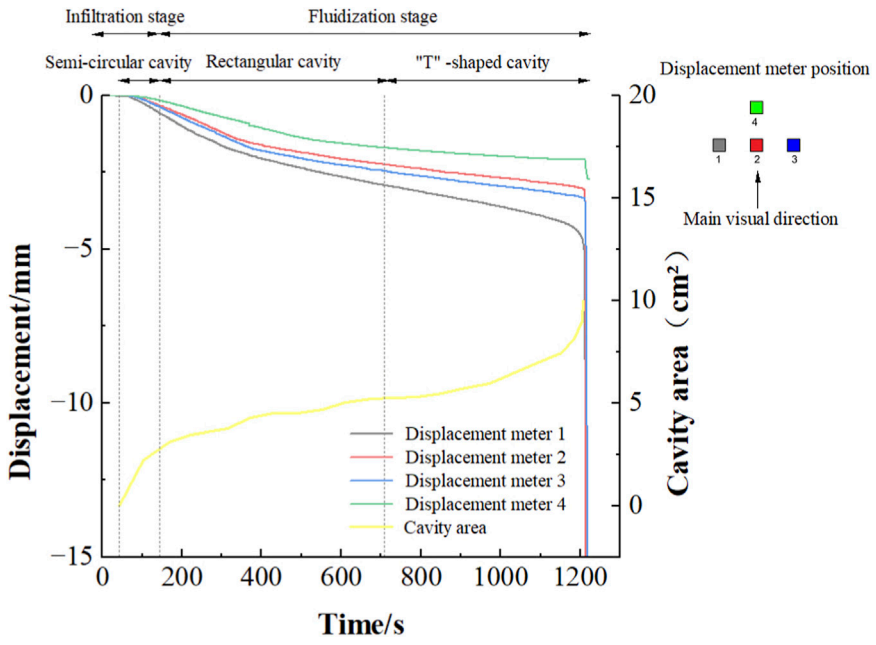

FIGURE 13
Comparison chart of ground subsidence monitoring data and underground cavity area (case 10).

TABLE 4 Test result table when the compactness is 20%.

Case	Cavity area (cm^2)	Settlement (mm)	Pipeline flow velocity (m/s)
Case 2	11.19	2.7	1.42
Case 3	12.97	3	1.5
Case 4	14.30	3.26	1.55
Case 5	15.61	3.51	1.62
Case 6	17.50	4.21	1.69

TABLE 5 Test result table when the flow velocity is 1.69 m/s.

Case	Cavity area (cm^2)	Settlement (mm)	Compactness of sand (%)
Case 6	9.99	3.06	20
Case 12	11.77	3.3	27.5
Case 18	14.64	3.76	35
Case 24	17.50	4.21	42.5

Due to the complexity of geological conditions, it is worth noting that the monitoring and warning models above is still conceptual and intended for preliminary guidance only. In further research and practical applications, it is recommended to apply the monitoring and warning model to high-risk areas of ground collapse, and implement warnings based on real-time data of ground subsidence obtained from monitoring. If it can be combined with intermittent underground cavity detection, it will be more accurate. Once the surface subsidence monitoring value exceeds the threshold determined by either of the above two formulas, the surface subsidence value has reached the dangerous area shown in Figure 15, and a ground collapse warning can be issued, and corresponding control measures should be taken.

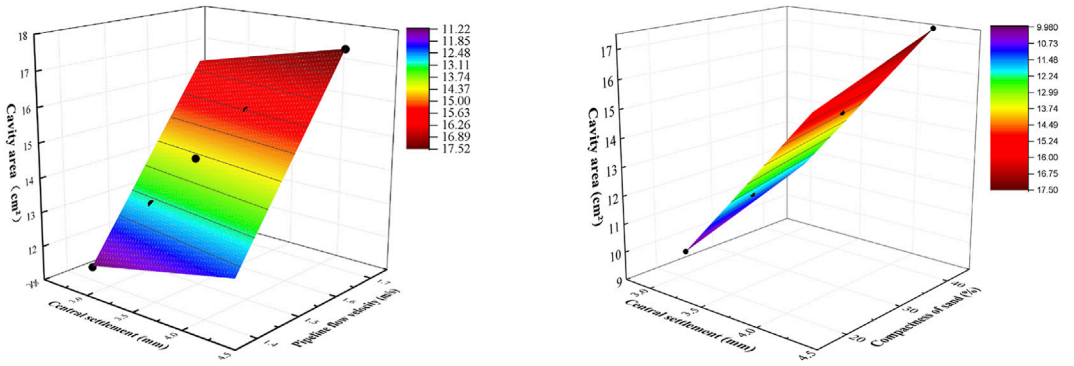

FIGURE 14
Fitting diagrams for the cavity area, subsidence, and pipeline flow velocity.

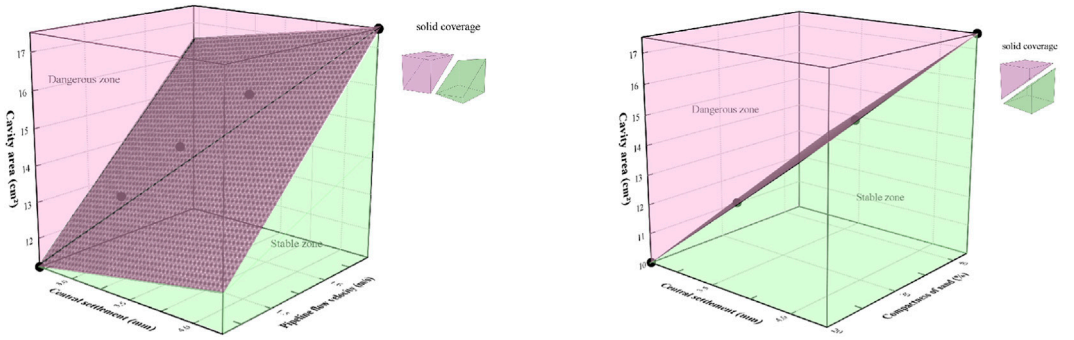

FIGURE 15
Warning map of ground collapse induced by leakage of pressure water pipe.

5 Conclusion

In this study, a series of pipeline leakage experiments was conducted to investigate the process, results, and critical conditions of ground collapse caused by pressurized hydraulic pipeline leakage. The key points are presented below.

1. Due to different combinations of compactness of sand and water flow velocity, water pipe leakage can lead to three different final states: infiltration disturbance, stable cavities, and fluidization failure.
2. Based on logarithmic regression analysis, the critical conditions and prediction model between the state of stable cavities and fluidized failure were obtained, which can be used for predicting ground collapse caused by pipeline leakage.
3. Based on the cone hypothesis, a regression analysis was conducted on the correlation between erosion angle and compactness of sand to obtain a prediction model for the scale (volume and area) of ground collapse caused by pipeline leakage, based on compactness of sand and the thickness of overlying soil.
4. A ground collapse early warning model was proposed based on the correspondence between surface subsidence monitoring data and the area of cavities in the soil during the experimental process.
5. The soil used for the experiment was river sand with particle sizes too large (>2 mm) or too small (≤0.075 mm) screened out. To reflect a more realistic soil condition, a wider range of soil types should be studied in the further research.

Data availability statement

The original contributions presented in the study are included in the article/supplementary material, further inquiries can be directed to the corresponding author.

Author contributions

LZ: Conceptualization, Funding acquisition, Methodology, Writing – original draft. QP: Conceptualization, Data curation, Investigation, Methodology, Writing – original draft. HS: Conceptualization, Investigation, Methodology, Writing – original draft. YW: Conceptualization, Methodology, Supervision, Validation, Writing – original draft, Writing – review and editing. QH: Supervision, Validation, Writing – review and editing. DZ:

Conceptualization, Supervision, Validation, Writing – review and editing.

Funding

The author(s) declared that financial support was received for this work and/or its publication. Zhejiang Provincial Basic Public Welfare Strategic Geological Special Fund Project (ShengZi 2024009). This fund supported the purchase of experimental equipment and the conduct of experiments in this study; Wenzhou Science and Technology Project (GK20250037). This fund supports the expenses and data analysis of experimental personnel in this study.

Conflict of interest

The author(s) declared that this work was conducted in the absence of any commercial or financial relationships that could be construed as a potential conflict of interest.

Generative AI statement

The author(s) declared that generative AI was not used in the creation of this manuscript.

Any alternative text (alt text) provided alongside figures in this article has been generated by Frontiers with the support of artificial intelligence and reasonable efforts have been made to ensure accuracy, including review by the authors wherever possible. If you identify any issues, please contact us.

Publisher's note

All claims expressed in this article are solely those of the authors and do not necessarily represent those of their affiliated organizations, or those of the publisher, the editors and the reviewers. Any product that may be evaluated in this article, or claim that may be made by its manufacturer, is not guaranteed or endorsed by the publisher.

References

Ahmad, S., Rizvi, Z., Arsalan Khan, M., Ahmad, J., and Wuttke, F. (2019). Experimental study of thermal performance of the backfill material around underground power cable under steady and cyclic thermal loading. *Mater. Today Proc.* 17, 85–95. doi:10.1016/j.matpr.2019.06.404

Ahmad, S., Rizvi, Z. H., Arp, J. C. C., Wuttke, F., Tirth, V., and Islam, S. (2021). Evolution of temperature field around underground power cable for static and cyclic heating. *Energies* 14, 8191. doi:10.3390/en14238191

Ahmad, S., Ahmad, S., Akhtar, S., Ahmad, F., and Ansari, M. A. (2025a). Data-driven assessment of corrosion in reinforced concrete structures embedded in clay dominated soils. *Sci. Rep.* 15, 22744. doi:10.1038/s41598-025-08526-w

Ahmad, S., Rizvi, Z. H., and Wuttke, F. (2025b). Unveiling soil thermal behavior under ultra-high voltage power cable operations. *Sci. Rep.* 15, 7315. doi:10.1038/s41598-025-91831-1

Alsabhan, A. H. (2021). The effect of opening shapes on the stability of underground tunnels: a finite element analysis. *Geomate* 21. doi:10.21660/2021.87.j2267

Cui, X., Li, J., Chan, A., and Chapman, D. (2014). Coupled DEM–LBM simulation of internal fluidisation induced by a leaking pipe. *Powder Technology* 254, 299–306. doi:10.1016/j.powtec.2014.01.048

Dai, Z., Peng, L., and Bao, Y. (2024). Model test investigation on the mechanism of ground collapse induced by underground hydraulic pipe leakage. *China J. Highw. Transp.* 37, 49–60. doi:10.19721/j.cnki.1001-7372.2024.10.005

Guarino, P. M., Santo, A., Forte, G., De Falco, M., and Niceforo, D. M. A. (2018). Analysis of a database for anthropogenic sinkhole triggering and zonation in the naples hinterland (southern Italy). *Nat. Hazards Dordr.* 91, 173–192. doi:10.1007/s11069-017-3054-5

Guo, J., Zhang, Y., Li, Y., Zhang, X., Zheng, J., Shi, H., et al. (2024). Model experimental study on the mechanism of collapse induced by leakage of underground pipeline. *Sci. Reports* 14, 17717. doi:10.1038/s41598-024-68824-7

Hermosilla, R. G. (2012). The Guatemala city sinkhole collapses. *Carbonates Evaporites* 27, 103–107. doi:10.1007/s13146-011-0074-1

Hou, C., Dong, M., and Pang, H. (2013). Huan-ping. Research on genesis and mechanics of land collapse in incompact soil. *J. Hefei Univ. Technol. Nat. Sci.* 36, 63–67.

Hu, Y.-H., B, Y.-C., and Xu, H.-J. (2016). Analysis of reasons for urban road collapse and prevention and control countermeasures in recent decade of China. *Highway* 61, 130–135.

Kuliczkowska, E. (2016). An analysis of road pavement collapses and traffic safety hazards resulting from leaky sewers. *Baltic J. Road Bridge Eng.* 11, 251–258. doi:10.3846/bjrbe.2016.29

Liu, J., Liu, H., and Wu, X. (2007). Mechanism and temporal-spatial distribution of ground collapse in guangzhou. *J. Catastrophology* 22, 62–65. doi:10.3969/j.issn.1000-811X.2007.04.014

Liu, J.-C., Wang, Z.-Y., Tan, Y., and Cao, Y.-C. (2024). Failure evolution and mechanism of ground collapse due to exfiltration of shallowly buried water pipeline. *Eng. Failure Analysis* 162, 108390. doi:10.1016/j.engfailanal.2024.108390

Mao, X., and Huang, S. (2014). Cause analysis of road collapse in Tianjin Municipality and its prevention and control countermeasures. *J. Nat. Disasters* 23, 218–226. doi:10.13577/j.jnd.2014.0627

Momeni, A., Piratla, K. R., Anderson, A., Chalil Madathil, K., and Li, D. (2023). Stochastic model-based leakage prediction in water mains considering pipe condition uncertainties. *Tunn. Underground Space Technology* 137, 105130. doi:10.1016/j.tust.2023.105130

Mukunoki, T., Kumano, N., Otani, J., and Kuwano, R. (2009). Visualization of three dimensional failure in sand due to water inflow and soil drainage from defective underground pipe using X-ray CT. *Soils Found.* 49, 959–968. doi:10.3208/sandf.49.959

Rizvi, Z. H., Mustafa, S. H., Sattari, A. S., Ahmad, S., Furtner, P., and Wuttke, F. (2020). "Dynamic lattice element modelling of cemented geomaterials," in *Advances in computer methods and geomechanics*. Editors A. Prashant, A. Sachan, and C. S. Desai (Singapore: Springer Singapore), 655–665. doi:10.1007/978-981-15-0886-8_53

Shi, Q., Wei, H., Tan, F., Zhou, J., and Zhu, J. (2022). Analysis of the characteristics and causes of urban ground subsidence disasters in shenzhen. *Bull. Geol. Sci. Technol.* 41, 123–129.

Tan, Y., and Long, Y.-Y. (2021). Review of cave-in failures of urban roadways in China: a database. *J. Perform. Constr. Facil.* 35, 1–20. doi:10.1061/(asce)cf.1943-5509.0001658

Tan, F., Tan, W., Yan, F., Qi, X., Li, Q., and Hong, Z. (2022). Model test analysis of subsurface cavity and ground collapse due to broken pipe leakage. *Appl. Sciences* 12, 13017. doi:10.3390/app122413017

Yuan, P. (2014). Study on collapse mechanism of soil subgrade of city roads by water erosion.

Yuan, X., Yan, Y., Li, X., Wang, T., and Ji, J. (2025). Discrete element simulation of ground collapse induced by buried sewage pipeline breakage and soil leakage. *Eng. Failure Analysis* 167, 108910. doi:10.1016/j.engfailanal.2024.108910

Zhang, Z., Mao, M., Pan, Y., Zhang, M., Ma, S., Cheng, Z., et al. (2022). Experimental study for joint leakage process of tunnel lining and particle flow numerical simulation. *Eng. Failure Analysis* 138, 106348. doi:10.1016/j.engfailanal.2022.106348

Zheng, G., Dai, X., and Zeng, C. F. (2016). Experimental and simplified model study of the development of ground settlement under hazards induced by loss of groundwater and sand. *Nat. Hazards* 82, 1869–1893. doi:10.1007/s11069-016-2275-3

Zhou, H., Liu, C., Wang, G., Kang, K., and Liu, Y. (2022). Study on drilling ground collapse induced by groundwater flow and prevention based on a coupled CFD-DEM method. *KSCE J. Civ. Eng.* 26, 2112–2125. doi:10.1007/s12205-022-1061-x

Zoueshtiagh, F., and Merlen, A. (2007). Effect of a vertically flowing water jet underneath a granular bed. *Phys. Review. E, Stat. Nonlinear, Soft Matter Physics* 75, 056313. doi:10.1103/PhysRevE.75.056313